doi.org/10.26434/chemrxiv.8246966.v2

Synthesis-Controlled Polymorphism, Magnetic and Electrochemical Properties of Li3Co2SbO6

Alex J. Brown, Brendan J. Kennedy, Chris D. Ling

Submitted date: 17/06/2019 • Posted date: 17/06/2019

Citation information: Brown, Alex J.; Kennedy, Brendan J.; Ling, Chris D. (2019): Synthesis-Controlled Polymorphism, Magnetic and Electrochemical Properties of Li3Co2SbO6. ChemRxiv. Preprint.

Li3Co2SbO6 is found to adopt two highly distinct structural forms: a hexagonal layered O3- LiCoO2 type phase with “honeycomb” 2:1 ordering of Co and Sb; and an orthorhombic superstructure of rock-salt type, isostructural with Li3Co2TaO6 but with the addition of significant Li/Co ordering. Pure samples of both phase scan be obtained by conventional solid-state synthesis from the same precursors, Li3SbO4 and CoO, by controlling particle size and reaction time. Both phases show relatively poor performance as lithium-ion battery cathode materials in their as-made states, but complex and interesting low-temperature magnetic properties. The honeycomb phase orders antiferromagnetically below TN = 14 K, but a positive Weiss constant θw = 18.1 K points to strong ferromagnetic interactions in the paramagnetic regime above TN; and isothermal magnetisation below TN shows evidence for a field-induced “spin-flop” transition at H ~ 0.7 T. The rock-salt type superstructure phase orders antiferromagnetically below TN = 112 K, then undergoes two more transitions at 80 K and 60, suggesting close competition between at least three ground states. Consistent with such competition, the Weiss constant θw = -181 K indicates some frustration, there is a strong field-cooled / zero field-cooled divergence below TN, and isothermal magnetisation shows it to be magnetically soft with low coercivity.

File list (3)

Li3Co2SbO6.pdf (2.14 MiB)	view on ChemRxiv • download file
HC.cif (0.97 KiB)	view on ChemRxiv • download file
RS.cif (1.67 KiB)	view on ChemRxiv • download file

Synthesis-controlled polymorphism, magnetic and electrochemical properties of $Li_3Co_2SbO_6$

Alex J Brown, Brendan J Kennedy and Chris D Ling*

School of Chemistry, The University of Sydney, Sydney 2006, Australia

Abstract

$Li_3Co_2SbO_6$ is found to adopt two highly distinct structural forms: a hexagonal layered O3-$LiCoO_2$ type phase with "honeycomb" 2:1 ordering of Co and Sb; and an orthorhombic superstructure of rock-salt type, isostructural with $Li_3Co_2TaO_6$ but with the addition of significant Li/Co ordering. Pure samples of both phase scan be obtained by conventional solid-state synthesis from the same precursors, Li_3SbO_4 and CoO, by controlling particle size and reaction time. Both phases show relatively poor performance as lithium-ion battery cathode materials in their as-made states, but complex and interesting low-temperature magnetic properties. The honeycomb phase orders antiferromagnetically below T_N = 14 K, but a positive Weiss constant θ_w = 18.1 K points to strong ferromagnetic interactions in the paramagnetic regime above T_N; and isothermal magnetisation below T_N shows evidence for a field-induced "spin-flop" transition at H ~ 0.7 T. The rock-salt type superstructure phase orders antiferromagnetically below T_N = 112 K, then undergoes two more transitions at 80 K and 60, suggesting close competition between at least three ground states. Consistent with such competition, the Weiss constant θ_w = -181 K indicates some frustration, there is a strong field-cooled / zero field-cooled divergence below T_N, and isothermal magnetisation shows it to be magnetically soft with low coercivity.

Introduction

Layered transition metal oxides of the type A_xMO_2, where A is an alkali metal and M is a transition metal, are among the most intensively studied class of solid-state compounds in recent years.[1] They are the dominant materials used as positive electrode (cathode) materials for Li-ion batteries due to their high performance combined with relative ease of synthesis, high stability and high melting points. They also display a wide variety of other fascinating physical phenomena. For example, Na_xCoO_2 shows interesting thermoelectric properties and favourable electrochemical properties for use as a positive electrode in Na-ion batteries;[2–4] and becomes superconducting ($T_c \sim 5$ K)[5,6] after intercalating water as $Na_{0.3}CoO_2 \bullet 1.4H_2O$.

The key structural motif of the A_xMO_2 oxides is hexagonal (or pseudo-hexagonal) layers of edge-sharing MO_6 octahedra, alternating with layers of A cations in either octahedral or trigonal coordination depending on the MO_6 layer stacking arrangement. Substituting 1/3 of the M sites with another element, M', can gives rise to ordered superstructures with the general formula $A_xM_2M'O_6$, where each $M'O_6$ octahedron is surrounded by six edge-sharing MO_6 octahedra to form "honeycomb" layers. The honeycomb arrangement is stabilised when the charge difference between M and M' is large but the size difference is relatively small: specifically, $M = Mg^{2+}$, Co^{2+}, Ni^{2+}, Cu^{2+}, Zn^{2+} and $M' = Sb^{5+}$ Bi^{5+} or Te^{6+}. The first reported $A_3M_2M'O_6$ honeycomb-type phases were $Li_3Zn_2SbO_6$ and $Li_3Zn_2BiO_6$ in 1990.[7] $Li_3Zn_2SbO_6$ has Zn^{2+}/Sb^{5+} octahedral honeycomb ordering with alternating metal layers separated by Li^+ layers. Since then, the number of known examples has expanded to include most of the combinations $A_3M_2M'O_6$ (A = Na, Li; M = Mg, Co, Ni, Cu, Zn; M' = Sb, Bi), $A_2M_2TeO_6$ (A = Li, Na, K; M = Co, Cu, Mg, Zn, Ni) and Li_4MTeO_6 (M = Co, Ni, Cu, Zn).[7–23]

However, the above $A_3M_2M'O_6$ stoichiometries do not always give rise to honeycomb-ordered phases. In some cases, the honeycomb phase competes with a rock-salt type ordered arrangement commonly referred to as an orthorhombic *Fddd* superstructure, of which the first reported example is $Li_3Co_2TaO_6$.[24] Examples of the *Fddd* phase include $Li_3M_2M'O_6$ (M = Ni, Co, Mg; M' = Nb, Ta, Sb) and Li_xMTeO_6 (M = Co, Ni; $2 \leq x \leq 3$).[24–27]

More recently, K^+ honeycomb tellurates $K_2M_2TeO_6$ (M = Ni, Mg, Zn, Co and Cu) have been synthesised and studied as rechargeable K-ion battery cathode materials.[28] $K_2Ni_2TeO_6$ can reversibly insert K^+ at voltages of ~4 V and has a discharge/charge capacity of ~ 70 mAh g^{-1}. It also shows very good ionic conductivity of 0.01 mS cm^{-1} at 298 K.[28]

Another significant area of interest in the honeycomb oxides has been their low-temperature magnetic properties. Hexagonal arrangements of magnetic *M* cations around a non-magnetic *M'* cation can lead to frustrated magnetic ground states; and the relatively long and weak inter-layer magnetic interactions means that the systems are pseudo-low dimensional and highly susceptible to competing quantum fluctuations.[29] Honeycomb oxides have been reported to show spin-glass behaviour and spin-flop transitions, in addition to a long-range-ordered 'zig-zag' antiferromagnetic (AFM) ground state that breaks hexagonal symmetry[8,12,13,29] in preference to the more intuitive Néel state that would preserve it. Finally, recent theoretical work suggests that Co^{2+} d^7 honeycomb compounds could stabilise Kitaev exchange and give rise to a quantum spin-liquid state.[30]

The present work concerns $Li_3Co_2SbO_6$, which is conspicuously absent from the literature on the $Li_3M_2SbO_6$ honeycomb-type phases. In particular there has not yet been any detailed structural or magnetic investigation of this phase in the literature. The only publicly available information about this phase comes from an XRD pattern deposited with the ICDD (Powder Diffraction File 00-58-637). The pattern was indexed to a *C*2/*m* unit cell (a common monoclinic distortion of the hexagonal honeycomb phases), but no further information was provided. Here, we report the solid-state synthesis, crystal structure, magnetism and basic electrochemical performance of $Li_3Co_2SbO_6$ in two polymorphs: an O3-type honeycomb phase; and an *Fddd* rock salt-type superstructure.

Experimental

$Li_3Co_2SbO_6$ was prepared using conventional solid-state methods. Starting materials were obtained from commercial suppliers. Li_3CO_3 (99.9%, Sigma-Aldrich) was dried at 120 °C prior to reaction to avoid moisture contamination. 5 g samples of Li_3SbO_4 precursor were prepared based on methods previously described in the literature.[31,32] Li_3CO_3 and Sb_2O_3 (99%, BDH Chemicals) were mixed in the relevant stochiometric ratios and ground with acetone using an agate mortar and pestle. The ground paste was dried before being pressed into a 20 mm pellet at ~35 Mpa. The pellet was then reacted at an initial temperature of 650 °C for 2 hours, before calcining at 950 °C for 12 hours. Li_3SbO_4 was obtained as a cream-coloured polycrystalline sample and characterised by X-ray diffraction (XRD). 5-6 g samples of CoO were synthesised from Co_3O_4 (99.9%, Sigma-Aldrich) by heating finely ground. Co_3O_4 as a loose powder at 1050 °C under flowing Ar in a tube furnace for 12 h. The resulting brown powder of CoO was characterised by XRD. 2-3 g samples of honeycomb

phase $Li_3Co_2SbO_6$ were prepared from a stochiometric 1:2 mixture of Li_3SbO_4 and CoO. The mixture was ground using an agate mortar and pestle before being pressed into a rod at ~40 Mpa using a hydrostatic press. The rod was placed in an alumina boat, heated to 1100 °C under flowing Ar at a rate of 6 °C/min, held at that temperature for 90 min then furnace-cooled to room temperature. These short reaction times were found to produce the most crystalline samples and minimise evaporation of Li. The resulting compound was a pinkish-red powder.

2-3 g samples of the rock salt-type superstructure phase of $Li_3Co_2SbO_6$ were prepared in a similar manner. Li_3SbO_4 and CoO were mixed with Li_3SbO_4 by ball-milling for 3 h at 400 rpm. The ball-milled mixture was then pressed into a rod at ~40 Mpa using a hydrostatic press. The rod was heated to 1100 °C, in an alumina boat under flowing Ar, at a rate of 8 °C/min. The temperature was held at 1100 °C for 3 h then furnace-cooled to room temperature. The resulting sample was a pink powder.

Polycrystalline samples were characterised by X-ray powder diffraction (XRD) on a PANalytical X'Pert Pro MPD, using non-monochromated Cu Kα radiation ($K\alpha_1$, λ = 1.5406 Å; $K\alpha_2$, λ = 1.5444 Å) with a Ni filter. Data were collected in Bragg-Brentano θ:2θ geometry, with a voltage of 45 kV and current of 40 mA, at a scanning rate of 0.045 2θ/s, typically over the range $5 < 2\theta < 90$ °2θ.

The rock salt-type superstructure phase of $Li_3Co_2SbO_6$ was further characterised by low-temperature XRD using a STOE Stadi P diffractometer with a Mo-$K_{\alpha1}$ source (λ = 0.7093 Å), monochromatised by (111) Ge. The sample was mounted on an Al-coated bronze sample holder. Temperatures were achieved using an Oxford Cryosystems PheniX with data measured to 12 K, in steps of 20 K with collection times of 3 h per step. Data were collected in the range $5 < 2\theta < 55$ ° using a Dectris MYTHEN2 1K microstrip detector.

Structures were refined using the Rietveld method as implemented in TOPAS (V5). The background was fit using a 8th order Chebychev polynomial. For the honeycomb phase preferred orientation (PO) was modelled using the spherical harmonics function (Järvinen, 1993) found in TOPAS.[33,34] The peaks were modelled using the pseudo-Voigt TCHZ function.

Magnetic susceptibilities were measured using a Quantum Design Physical Properties Measurement System (PPMS). Temperature-dependent DC magnetic susceptibility measurements were taken under zero field-cooled (ZFC) and field-cooled (FC) conditions

over the range 2-300 K, in an applied field of 0.1 T. Isothermal field-dependent magnetisation data were collected to ± 3 T at constant temperatures.

Both $Li_3Co_2SbO_6$ phases were tested as Li-ion battery cathode materials. Composite electrodes were prepared by mixing with carbon black and polyvinylidene fluoride (PVDF) binder (80:10:10 wt%) and casting onto an aluminium foil current collector. Coin cells were made in an Ar-filled glovebox, with 1 M $LiPF_6$ in ethylene carbonate and diethyl carbonate (1:1 volume ratio) used as the electrolyte. Li metal was the counter electrode, separated from the $Li_3Co_2SbO_6$ electrode by a fibre glass separator. Electrochemical performance of the coin-cells was tested with a Neware BTS 4000 battery cycler, at 25 °C, with a constant current of 0.04 mA and voltage ranging from 2 to 4.2 V.

Results and Discussion

Synthesis

Initial attempts to prepare $Li_3Co_2SbO_6$ using a solid state method similar to that described for the Na analogue, $Na_3Co_2SbO_6$, were unsuccessful.[8] An alternative synthesis route was developed where the precursor Li_3SbO_4 was reacted with freshly prepared CoO.[31,32] The presence of fully oxidised Sb^{5+} in Li_3SbO_4 (vs. Sb^{3+} in the conventional reagent Sb_2O_3) allowed us to carry out the reaction under Ar flow, preventing further oxidation of Co^{2+}. Shorter reaction times at higher temperatures were found to favour formation of the honeycomb phase. Longer reaction times and/or ball-milling prior to heating were found to favour formation of the rock-salt superstructure phase.

Structural refinements

The structure of each $Li_3Co_2SbO_6$ phase was analysed by Rietveld-refinement against XRD data. The honeycomb phase was indexed in the monoclinic space group *C*2/*m*, isostructural with $Na_3Co_2SbO_6$, which has an O3-type layer stacking arrangement. The free *y* coordinate for Li2 was initially fixed to the value from the $Na_3Co_2SbO_6$ starting model,[8] due to the relative insensitivity of XRD data to light Li atoms, and refined in the final cycles. Li2 did not move, within error, from its position in the initial $Na_3Co_2SbO_6$ model. A trace amount of the rock salt-type superstructure phase (the structure of which is described below) was included in the refinement. The final Rietveld fit is shown in Figure 1 and the refined structure in Figure 2. Details of the refinement and the refined structure are given in Table 1, with selected bond data including bond valence sums (BVS)[35] in Table 2. A crystallographic

information file (CIF) for the final refined structure is available as Supplementary Information.

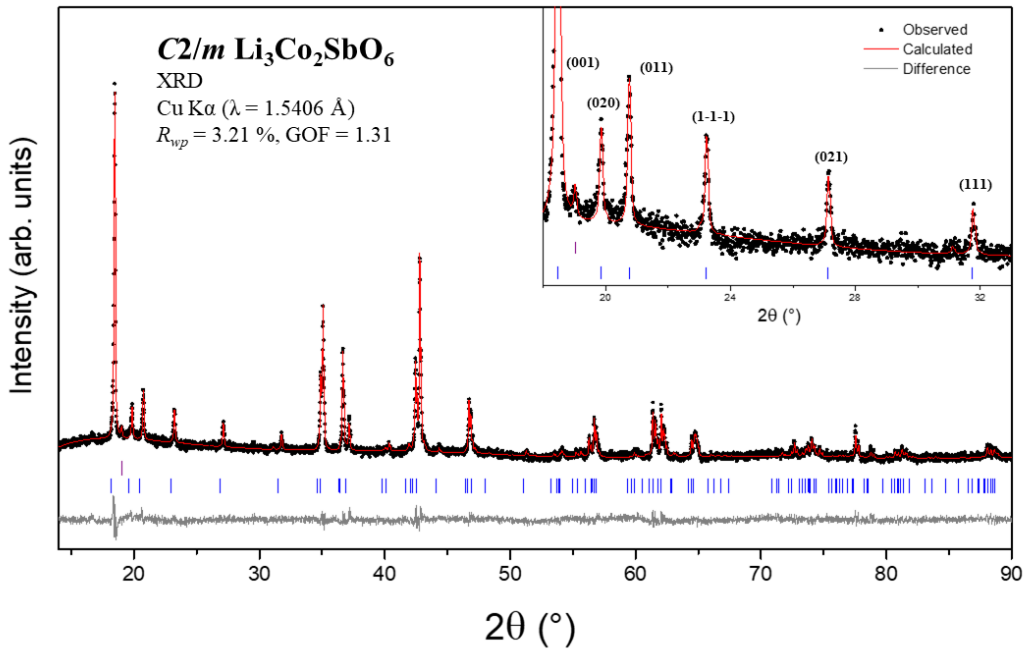

***Figure 1**: Rietveld refinement against XRD data (λ= 1.5406Å) for the C2/m honeycomb phase of $Li_3Co_2SbO_6$ at room temperature. Black circles are experimental data, the red line is the calculated pattern and the grey line is the difference. Bragg peaks are indicated by blue tick marks; the upper purple tick mark at 19 ° indicates the sole observed peak from a very small fraction of the rock salt-type superstructure phase. The inset highlights peaks due to Co:Sb honeycomb superlattice ordering, with Miller indices in parentheses.*

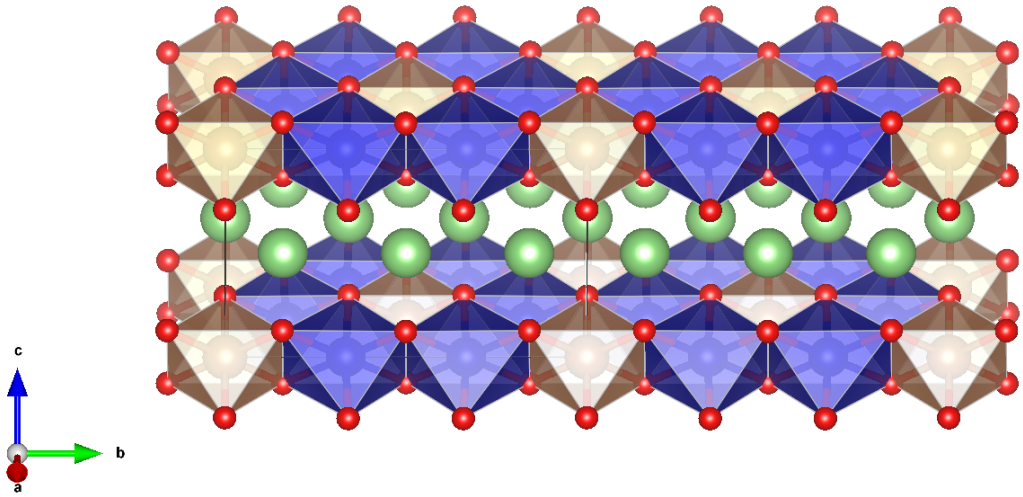

***Figure 2** Crystal structure of the C2/m O3-type honeycomb phase of $Li_3Co_2SbO_6$. CoO_6 octahedra are blue, SbO_6 octahedra are bronze, O atoms are red and Li atoms are green.*

Table 1: Unit cell dimensions, fractional coordinates and isotropic displacement parameters for the honeycomb phase of $Li_3Co_2SbO_6$, from Rietveld-refinement against XRD data. Superscript symbols indicate constraints.

Honeycomb $Li_3Co_2SbO_6$			**Crystal system**		**Space Group**		
GOF = 1.31, R_{wp} = 3.21%			Monoclinic		*C*2/*m*		
Radiation	**T (K)**	**a (Å)**	**b (Å)**	**c (Å)**	**β (°)**	**Volume (Å^3)**	
Cu Kα	298	5.2717(6)	9.0871(10)	5.2039(6)	110.1553(14)	234.02(5)	
Atom	**x**		**y**	**z**	**Occ.**	**B_{iso}(Å^2)**	**Wyckoff**
Co	0		2/3	0	1	0.3(2)	4*g*
Sb	0		0	0	1	0.2(2)	2*a*
O1	0.274(3)		0 348(2)	0.772(5)	1	0.9(4)†	8*j*
O2	0.246(4)		1/2	0.225(9)	1	0.9(4)†	4*i*
Li1	0		1/2	1/2	1	0.5(2)‡	2*d*
Li2	1/2		0.330(9)	1/2	1	0.5(2)‡	4*h*

Table 2: Selected interatomic distances (Å) and bond valence sums (BVS) for the honeycomb phase of $Li_3Co_2SbO_6$ at room temperature.

Co–O1 (x2)	2.138(6)	Li1–O1 (x4)	2.142(8)
Co–O1 (x2)	2.168(14)	Li1–O2 (x2)	2.239(18)
Co–O2 (x2)	2.075(10)	Average	2.17(2)
Average	2.127(18)	BVS (Li1)	0.8
BVS (Co)	1.9	Li2–O1 (x2)	2.147(13)
Sb-O1 (x4)	1.937(6)	Li2–O1 (x2)	2.30(6)
Sb-O2 (x2)	2.059(19)	Li2–O2 (x2)	2.22(6)
Average	1.98(4)	Average	2.22(2)
BVS (Sb)	5.1	BVS (Li2)	0.9

The honeycomb phase of $Li_3Co_2SbO_6$ has a smaller unit cell than that of $Na_3Co_2SbO_6$, with volumes of 234.02(5) and 266.43(18) Å^3 respectively. The difference in unit cell dimensions is most pronounced along the layer-stacking *c* axis (5.637(2) and 5.2717(6) Å), consistent

with the larger ionic radius of Na^+ vs. Li^+ (1.02 vs. 0.76 Å). The superlattice reflections due to 2:1 Co:Sb honeycomb ordering are sharp, demonstrating the absence of appreciable stacking faults.[22,36,37] Calculated BVS for the cations are all very close to their nominal values, further validating the structural changes from the $Na_3Co_2SbO_6$ starting model.

The rock salt-type superstructure phase was indexed in the orthorhombic space group *Fddd* and is isostructural with $Li_3Co_2TaO_6$.[24] For the structural refinements it was assumed that each cation site was fully occupied. The free *z* coordinate for Li1 was initially fixed at the value from the $Li_3Co_2TaO_6$ starting model, due to the relative insensitivity of XRD to light Li atoms,[24] and only refined in the last refinement cycles. Li1 was found to move only slightly from its position in the $Li_3Co_2TaO_6$ model, improving the fit from R_{wp} = 23.57%, GOF = 1.66 to R_{wp} = 22.67%, GOF = 1.59 in the final refinement. The final Rietveld fit is shown in Figure 3 and a representation of the structure in Figure 4. Details of the refinement and the refined structure are given in Table 3, with selected bond data including BVS in Table 4. A CIF for the final refined structure is available as Supplementary Information.

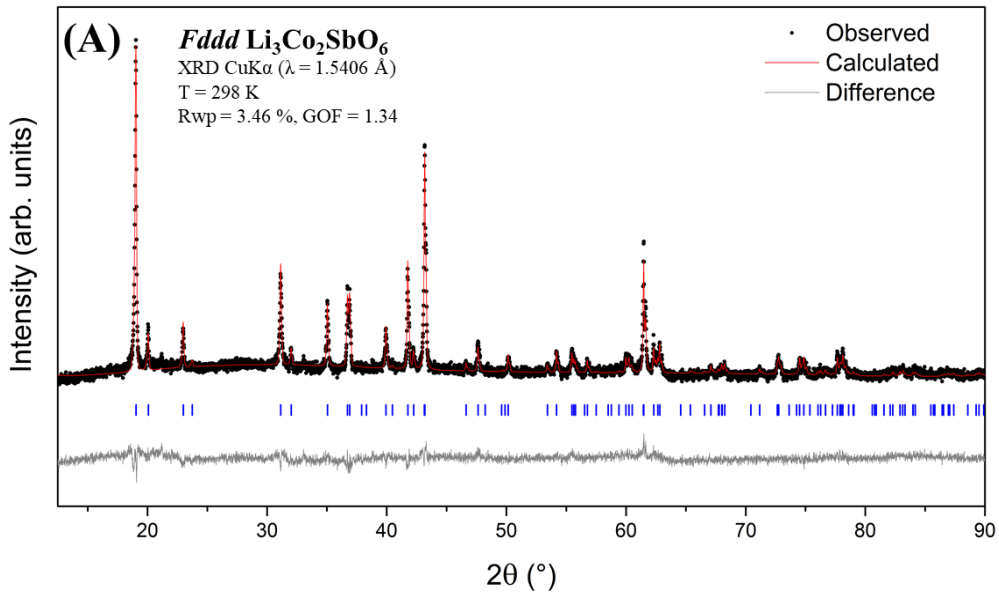

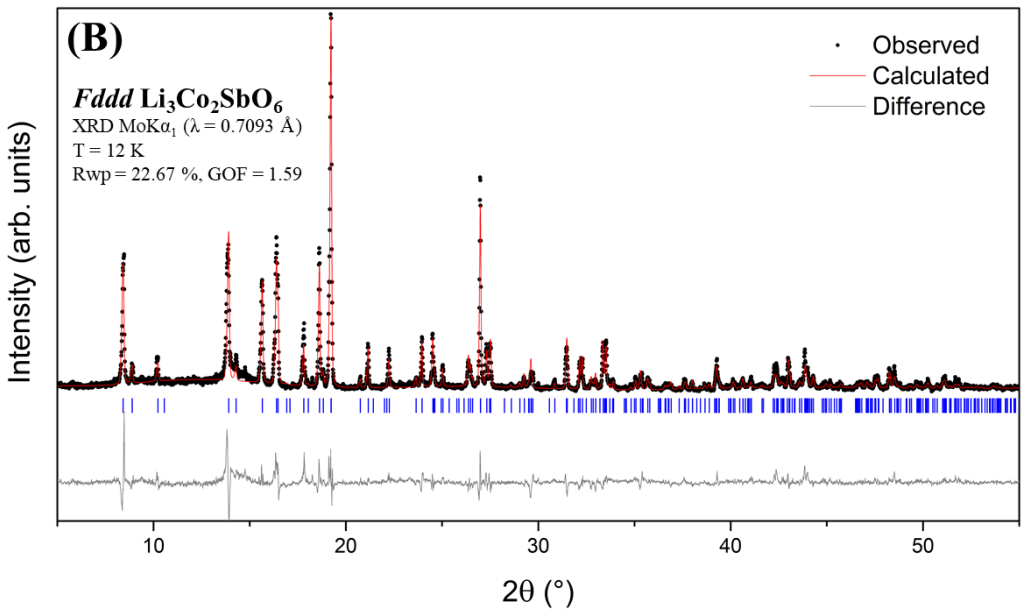

Figure 3: *Rietveld refinement of the Fddd rock salt-type superstructure phase of $Li_3Co_2SbO_6$ against XRD data from (A) a Cu Kα source (λ= 1.5418 Å) at 298 K and (B) a Mo $Kα_1$ source (λ= 0.7093 Å) at 12 K under vacuum. Observed data are black circles, the calculated fit is a red line and the difference is a grey line. Blue tick marks indicate Bragg reflections.*

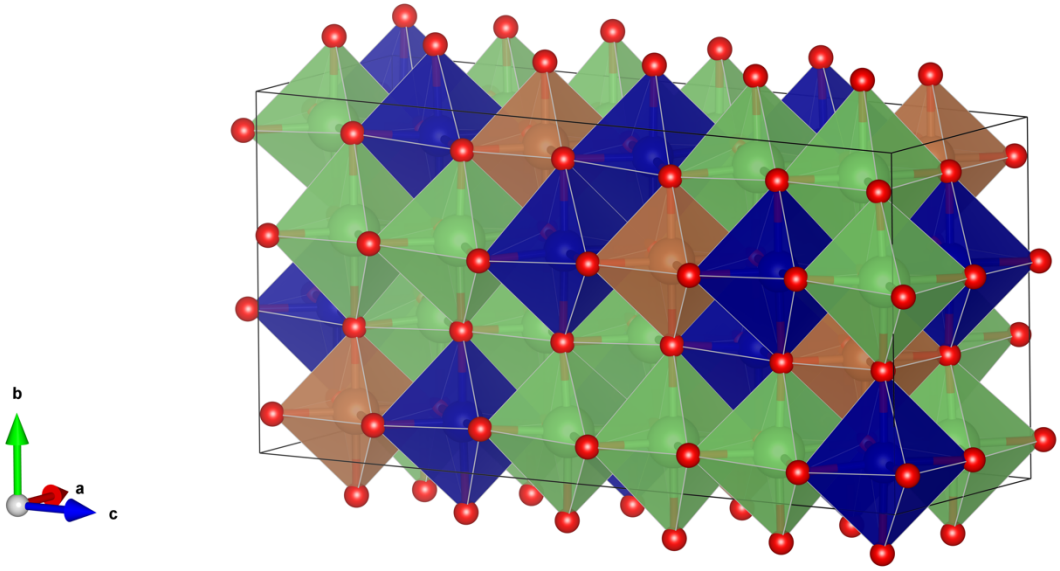

Figure 4 *Crystal structure of the Fddd rock salt-type superstructure phase of $Li_3Co_2SbO_6$. Co atoms are blue, Li atoms are green, Sb atoms are bronze and O atoms are red.*

Table 3 Unit cell dimensions, fractional coordinates, occupancies and isotropic displacement parameters for the rock salt-type superstructure phase of $Li_3Co_2SbO_6$, from Rietveld-refinement against XRD data at 12 K; and unit cell dimensions only (in italics) from Rietveld-refinement against XRD data at 298 K Superscript symbols indicate constraints.

Rock salt-type superstructure $Li_3Co_2SbO_6$				**Crystal system**		**Space Group**	
				Orthorhombic		*Fddd*	
Radiation	**T (K)**	**a (Å)**	**b (Å)**	**c (Å)**	**α= β=γ (°)**	**Volume (Å^3)**	
Cu Kα	*298*	*5.937(2)*	*8.703(2)*	*17.944(5)*	*90*	*927.4(4)*	
Mo $K\alpha_1$	12	5.918(2)	8.666(4)	17.884(7)	90	917.1(6)	
Atom		**x**	**y**	**z**	**Occ.**	**B_{iso}(Å^2)**	**Wyckoff**
Sb		1/8	1/8	1/8	1	0.2(1)	8*a*
Co1		1/8	1/8	0.2934(2)	1	0.3(1)	16*g*
Li1		1/8	5/8	0.2907(2)	1	1.0(4)	16*g*
Li2		1/8	5/8	1/8	0.82(4)	1.0(3)‡	8*b*
Co2		1/8	5/8	1/8	0.18(4)	1.0(3)‡	8*b*
O1		1/8	0.358(2)	1/8	1	0.40(15)†	16*f*
O2		0.1156(17)	0.377(2)	0.2954(7)	1	0.40(15)†	32*h*
GOF = 1.34, R_{wp} = 3.46% (Cu Kα); GOF = 1.59, R_{wp} = 22.67% (Mo $K\alpha_1$)							

Table 4 Selected interatomic distances (Å) and bond valence sums (BVS) for the rock salt-type superstructure phase of $Li_3Co_2SbO_6$ at 12 K.

Co1–O1 (x2)	2.0841(7)	Li1–O1 (x2)	2.118(7)
Co1–O2 (x2)	2.132(7)	Li1–O2 (x2)	2.1506(3)
Co1–O2 (x2)	2.186(3)	Li1–O2(x2)	2.174(7)
Average	2.134(4)	Average	2.15(4)
BVS (Co1)	1.8	BVS (Li2)	0.9
Sb-O1 (x2)	2.014(7)	Co2/Li2–O1 (x2)	2.316(14)
Sb-O2 (x4)	2.017(14)	Co3/Li2–O2 (x4)	2.094(7)
Average	2.016(14)	Average	2.17(5)
BVS (Sb)	4.5	BVS (Co2/Li2)	1.7/0.9

In this rock salt-type superstructure phase, SbO_6 octahedra share 12 edges with (Li,Co)O_6 octahedra. Placing Sb on the 8*a* Wykoff site maximises Sb–Sb distances to minimise electrostatic repulsion between Sb^{5+} cations. Li and Co are distributed over three crystallographically independent sites with varying Li:Co contents, all of which were refined. The 8*b* site is the most distorted of these, with the longest *M*-O bond distances, and was mostly occupied by Li with a small refined fraction of Co; while the two 16*g* sites were fully occupied by Co or Li within the standard deviations of the refinement, and were fixed as such. This is a notable departure from the starting model of $Li_3Co_2TaO_6$, which had Ta on the 8*a* site but a statistical occupancy of all three Li/Co sites.[24] Calculated BVS for the cations are reasonable, all falling within 10% of their nominal values with the exception of the small fraction of Co2 (BVS = 1.7+) on the mixed site dominated by Li2 (BVS = 0.9+). Note that the refined occupancies suggest a slightly Co-rich composition $Li_{2.82(7)}Co_{2.18(7)}SbO_6$. Given that this non-stoichiometry is only barely statistically significant, we will continue to refer to the phase as $Li_3Co_2SbO_6$, except where that non-stoichiometry is potentially significant (as in the discussion of magnetic properties, below).

Putting these results in a broader context, we note here that $Li_3Ni_2SbO_6$ has also been reported in a rock salt-type superstructure phase.[24] However, Nalbandyan and co-workers reported that they were unable to reproduce this despite their comprehensive work on the structure and magnetism of the honeycomb phase of the same stoichiometry,[9] and we were also unsuccessful in preparing this using either conventional reagents or a Li_3SbO_4 precursor. This reinforces the precise synthetic conditions required to control the balance between phases in these systems. More recently, $Li_3Co_{1.06}TeO_6$ was reported to crystallise in an orthorhombic *Fddd* space group with similar unit cell dimensions to other $Li_3M_2M'O_6$ rock salt-type superstructures,[27] but with Co^{2+} and Co^{3+} mixed valence states.

Magnetic properties

Temperature-dependent magnetic susceptibility data for the honeycomb phase of $Li_3Co_2SbO_6$ show an AFM ordering transition at a Néel temperature T_N = 14 K (Figure 5). There was no significant divergence between data collected under zero field-cooled (ZFC) and field-cooled (FC) conditions using an applied field of 0.1 T A Curie-Weiss fit to ZFC data over the range 150-300 K yielded a Weiss constant θ_w = 18.1 K and an effective magnetic moment of μ_{eff} = 5.04 μ_B per Co^{2+} ion. The latter value is consistent with high-spin Co^{2+} (d^7, S=3/2, μ_{so} = 3.87 μ_B), with an unquenched orbital contribution in a $^4T_{1g}$ (using the octahedral notation) ground

state, and is comparable to $\mu_{eff} = 5.22\ \mu_B$ reported for $Na_3Co_2SbO_6$.[1] The small deviation in susceptibility observed around 75-80 K is due to a trace amount of rock salt-type superstructure phase (the magnetic properties of which are described below). The values $T_N = 14$ K, $\theta_w = 18.1$ K for $Li_3Co_2SbO_6$ can be compared to $\theta_w = 8$ K and $T_N = 15$ K for $Li_3Ni_2SbO_6$,[4,21,22] and $T_N = 8.3$ K, $\theta_w = 2.2$ K for $Na_3Co_2SbO_6$. In all cases, the positive Weiss constants θ_w indicate the presence of significant ferromagnetic contributions above the AFM transition temperature.

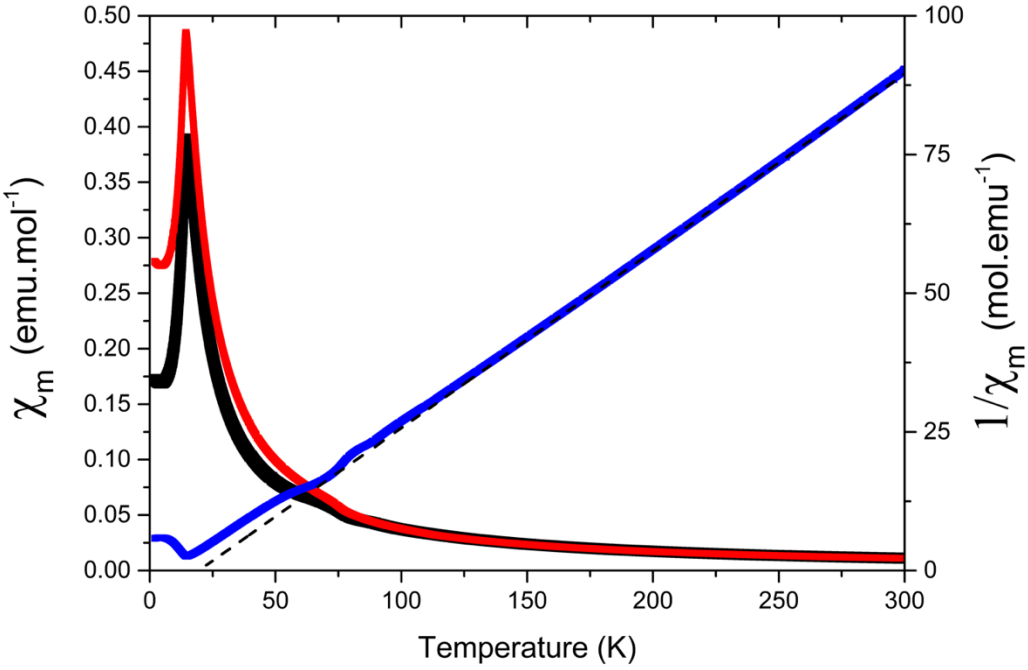

***Figure 5**: Temperature-dependent DC magnetic susceptibility (χ_m) and inverse magnetic susceptibility ($1/\chi_m$) as functions of temperature for the honeycomb phase of $Li_3Co_2SbO_6$, using an applied field of 0.1 T. The ZFC curve is black, the FC curve is red, and the inverse susceptibility is blue. The dotted black line shows the Curie-Weiss fit to the ZFC inverse susceptibility.*

Field-dependent magnetisation data for the honeycomb phase of $Li_3Co_2SbO_6$ were collected over the field range $-3\ T \leq H \leq 3\ T$ (Figure 6). At T = 20 K (above T_N), the behaviour is close to linear. At 2 K (below T_N), a metamagnetic transition is apparent at H = ~ 0.7 T. Other honeycomb oxides have been reported to undergo similar field-induced transitions, e.g.: $Na_3Co_2SbO_6$ has a magnetisation shoulder above H = 1 T, which has been attributed to a field-induced spin-flop transition;[8,13] $Na_2Co_2TeO_6$ has an upturn in magnetisation at ~ 5 T;[13,29,38] and $Na_3Ni_2BiO_6$ shows evidence of transition(s) from 4-7 T depending on

measurement temperature.[17] These results collectively underline the finely balanced and competing/frustrated nature of magnetic exchange in honeycomb antiferromagnets.

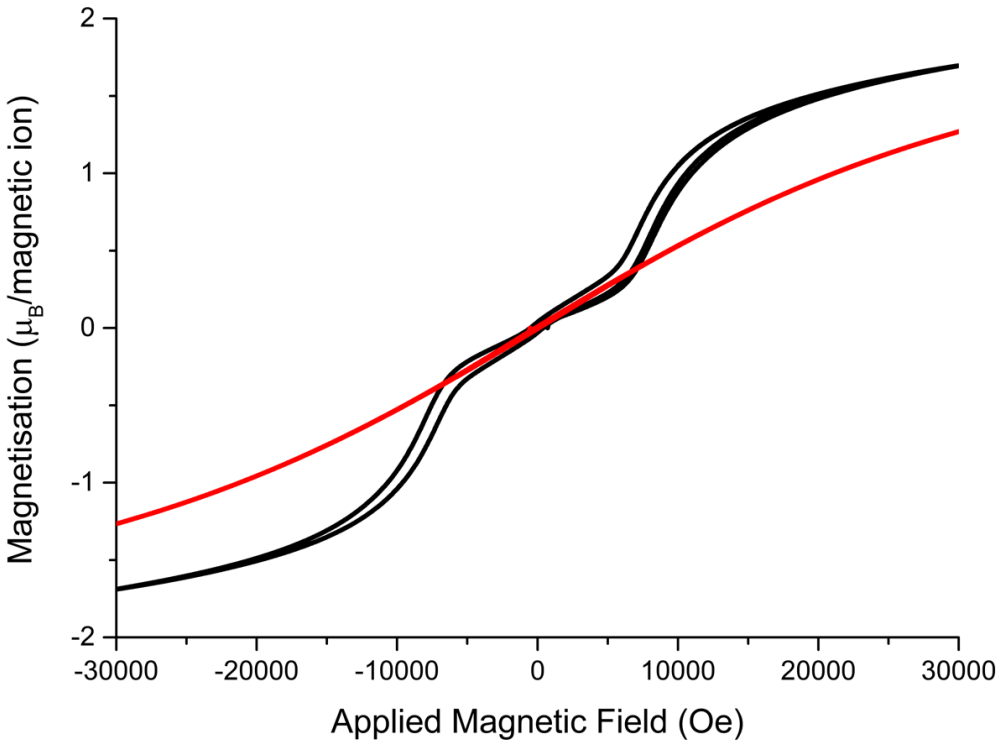

Figure 6: *Field-dependent magnetisation of the honeycomb phase of $Li_3Co_2SbO_6$ at 2 K (black) and 20 K (red), below and above T_N = 14.5 K, respectively.*

Temperature-dependent magnetic susceptibility data for the rock-salt superstructure phase of $Li_3Co_2SbO_6$ under ZFC conditions show a pronounced AFM transition on cooling through T_N = 113 K followed by more transitions at 80 K and 60 K (Figure 7). Noting that no impurity phases were evident in XRD data, the series of transitions suggests close competition between at least three ground states in this compound. A Curie-Weiss fit to the ZFC data for T > 160 K yields μ_{eff} = 5.06 μ_B, slightly larger than for the honeycomb phase of $Li_3Co_2SbO_6$. Taking into account the slight refined non-stoichiometry of the sample, $Li_{2.82}Co_{2.18}SbO_6$, the expected spin-only moment is either μ_{so} is either 3.52 μ_B (HS Co^{2+} and LS Co^{3+}) or 3.97 μ_B (HS Co^{2+} and HS Co^{3+}). In either case, there appear to be significant contributions from an unquenched orbital component, as is typical for HS Co^{2+} oxides. The highly negative Weiss constant θ_w = -181 K indicates dominant AFM exchange. The FC data strongly diverge from the ZFC data below T_N, with the applied field of 0.1 T appearing to be sufficient to induce an FM state.

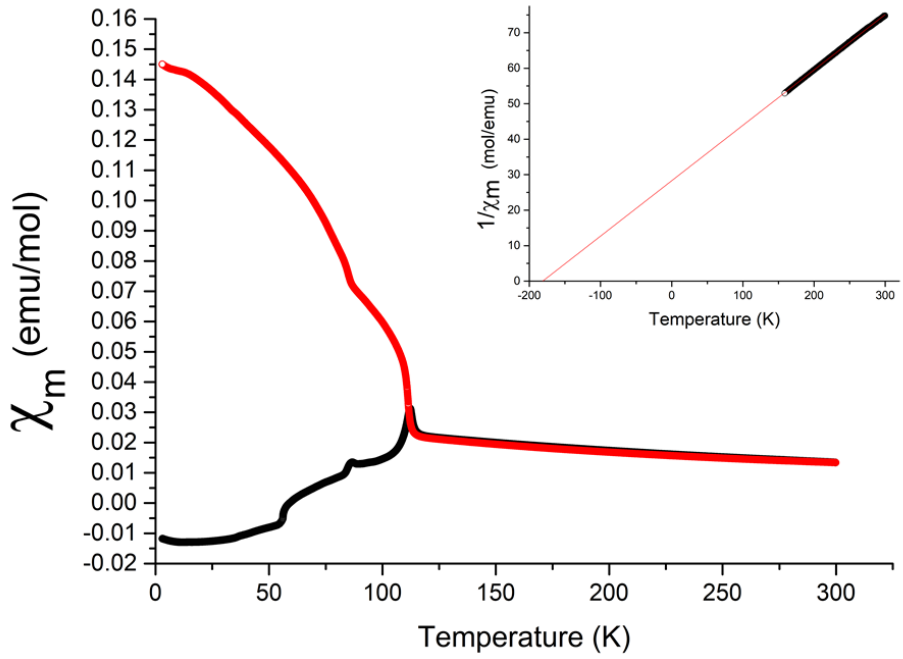

Figure 7: *Magnetic susceptibility as a function of temperature for the rock salt-type superstructure phase of $Li_3Co_2SbO_6$ in an applied field of 0.1 T. ZFC data are black and FC data are red. The inset shows the Curie-Weiss fit to ZFC inverse susceptibility above 160 K.*

Field-dependent magnetisation data for the rock-salt superstructure phase of $Li_3Co_2SbO_6$ were collected over a field range -3 T ≤ H ≤ 3 T (Figure 8) at T = 2 K and 90 K. Both data sets show predominantly AFM behaviour with a narrow hysteresis opening, but only the 2 K data show a (small) remanent magnetisation. The magnetisation is approximately two orders of magnitude smaller than for the honeycomb phase at the same fields.

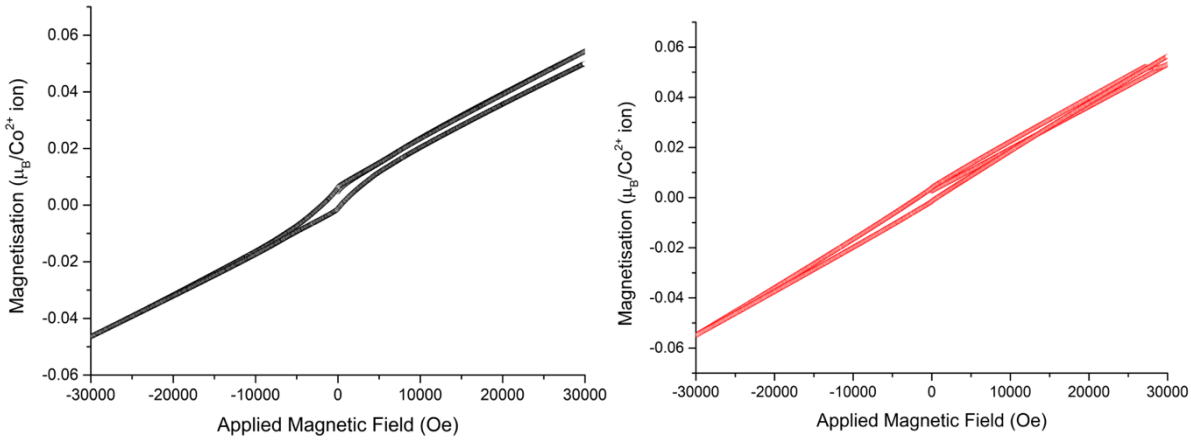

Figure 8: *Field-dependent magnetisation data for the rock salt-type superstructure phase of $Li_3Co_2SbO_6$ at 2 K (black) and 90 K (red).*

Electrochemical properties

The honeycomb and rock salt-type superstructure phases of $Li_3Co_2SbO_6$ were both tested as active positive electrode (cathode) materials in Li-ion coin cell batteries. Charge and discharge cycles are shown in Figures 9 and 10. Upon the first charge to 4.2 V, the honeycomb phase has a capacity of 32 mAh/g, while the rock salt-type superstructure phase has a capacity of 20 mAh/g. These low capacities fade after the first cycle, to 3.4 mAh/g and 3.7 mAh/g, respectively, and continue to decrease with each subsequent cycle. Note that the stoichiometry $Li_3Co_2SbO_6$ gives a calculated theoretical capacity of 75.2 mAh/g based on Co^{2+}/Co^{3+} redox alone, or up to 150.4 mAh/g if Co^{2+}/Co^{4+} redox is permitted.

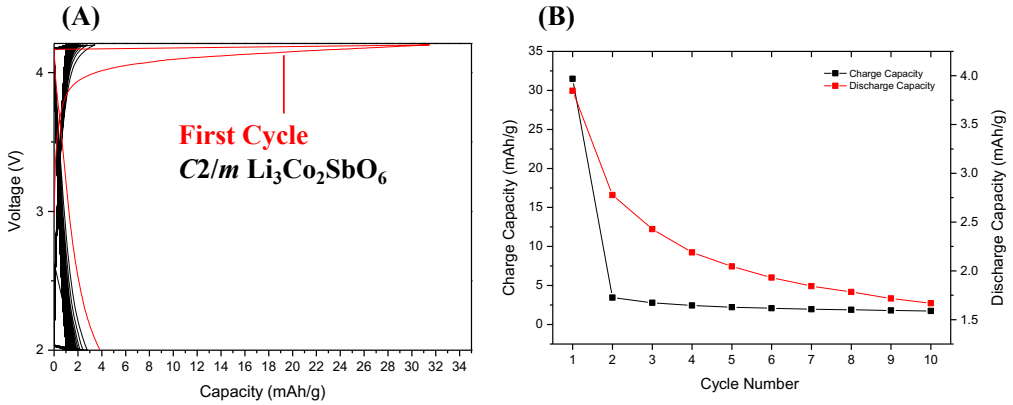

Figure 9 *(A) Charge/discharge voltage profiles of honeycomb-type $Li_3Co_2SbO_6$, with the first cycle in red and the next 99 cycles in black. (B) Capacity retention of charge (black) and discharge (red) for the first 10 cycles.*

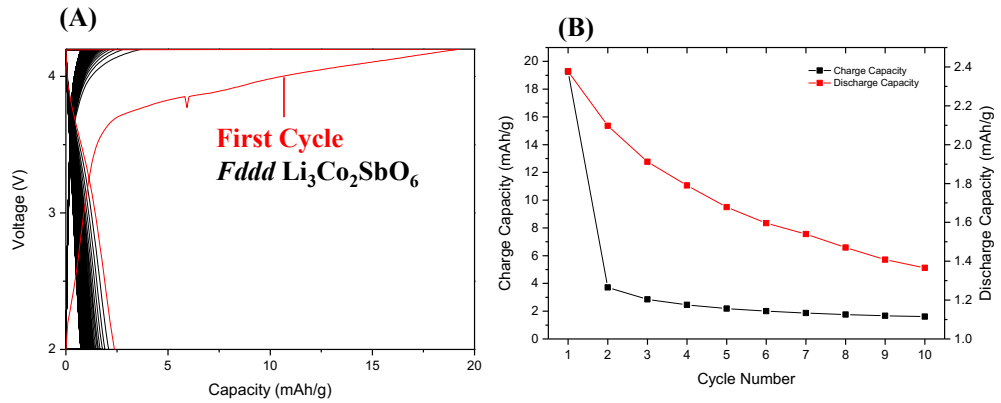

Figure 10: *(A) Charge/discharge voltage profiles for the rock salt-type superstructure phase of $Li_3Co_2SbO_6$, with the first cycle in red and the next 99 cycles in black. (B) Capacity retention of charge (black) and discharge (red) for the first 10 cycles.*

The capacity is inferior to a number of other honeycomb oxides, notably the Ni compounds. For example, $Na_3Ni_2SbO_6$ has been shown to have reversible capacities between 110-130 mAh/g with 70% retention over 500 cycles.[39,40] Similarly, $Na_2Ni_2TeO_6$ reversible capacity of 110 mAh/g.[41] Of the Li compounds, Li_4NiTeO_6 has a reversible capacity of 110-120 mAh/g.[42,43] However, the closest analogue to $Li_3Co_2SbO_6$ for which electrochemical data have been reported, $Li_3Ni_2BiO_6$, has a similarly low capacity of 22 mAh/g.[44]

Conclusions

$Li_3Co_2SbO_6$ can be prepared by conventional solid-state synthesis from pre-prepared Li_3SbO_4 and CoO. These precursor phases were found to be necessary so that Sb and Co would be present in their desired oxidation states (Sb^{5+} and Co^{2+}, at the upper and lower ends of their normal ranges in oxides, respectively) prior to reaction under a protective Ar flow. Two distinct phases can be obtained, even at the same temperature (1100 °C). Short reaction times and conventional grinding yield a layered honeycomb phase isostructural with $Na_3Co_2SbO_6$, while long reaction times and/or ball-milling prior to pelletising and heating yield a rock salt-type superstructure phase isostructural with $Li_3Co_2TaO_6$ (but with significant Li/Co ordering). Both phases are challenging to make as pure samples: the honeycomb phase, because it has a very narrow range of thermodynamic stability between the minimum required synthesis temperature and the transition to the rock salt-type superstructure phase; and the rock salt-type superstructure phase, because it loses Co to become non-stoichiometric at the synthesis temperature. Future work using low-temperature *chimie douce* synthetic routes may help address these challenges, but at the expense of crystallinity, which was the priority in the present work aimed at solving and refining the fully ordered structures.

Neither phase shows promising electrochemical performance as lithium-ion battery cathode in their as-made states, although it may be possible to improve this in the future by ball-milling to micron scale before casting onto Al foil, to increase surface area.

Both phases show complex and interesting low-temperature magnetism. For the layered honeycomb phase, temperature-dependent magnetic susceptibility data indicate long-range AFM ordering below T_N = 14 K, but a positive Weiss constant θ_w = 18.1 K points to strong FM interactions in the paramagnetic regime above T_N; and isothermal magnetisation below T_N shows evidence for a field-induced "spin-flop" transition at H ~ 0.7 T. Future temperature- and field-dependent neutron diffraction experiments will be worthwhile, to see

where the behaviour of this phase sits and how it contributes to the complex magnetic phase diagram of these frustrated honeycomb oxides.

The rock-salt type superstructure phase also undergoes long-range AFM order, at the significantly higher T_N = 112 K, but in this case with a strongly negative Weiss constant θ_w = -181 K that points to somewhat frustrated AFM intersections in paramagnetic regime. At lower temperatures, it undergoes two more transitions at 80 K and 60, suggesting that there are at least three competing ground states. Strong FC/ZFC divergence, and soft hysteresis in isothermal magnetisation, below T_N suggest a fine balance between local AFM and FM exchange interactions. As for the honeycomb phase, both temperature- and field-dependent neutron diffraction measurements (preferably on single crystals, which are not presently available) will be required to unravel this complex behaviour.

Supplementary Information

Crystallographic information files (CIFs) for the final refined structures of the honeycomb (HC.cif) and rock salt-type superstructure (RS.cif) phases of $Li_3Co_2SbO_6$.

Acknowledgements

CDL and BJK received funding for this work from the Australian Research Council – Discovery Projects. AJB received funding from the Australian Institute for Nuclear Science and Engineering – AINSE Honours Scholarships.

References

(1) Delmas, C.; Fouassier, C.; Hagenmuller, P. Structural Classification and Properties of the Layered Oxides. *Phys. BC* **1980**, *99* (1–4), 81–85.

(2) Delmas, C.; Braconnier, J.; Fouassier, C.; Hagenmuller, P. Electrochemical Intercalation of Sodium in Na_xCoO_2 Bronzes. *Solid State Ion.* **1981**, *3–4*, 165–169.

(3) Berthelot, R.; Carlier, D.; Delmas, C. Electrochemical Investigation of the P2–Na x CoO_2 Phase Diagram. *Nat. Mater.* **2011**, *10* (1), 74–80.

(4) Shacklette, L. W. Rechargeable Electrodes from Sodium Cobalt Bronzes. *J. Electrochem. Soc.* **1988**, *135* (11), 2669.

(5) Seibel, E. M.; Roudebush, J. H.; Ali, M. N.; Ross, K. A.; Cava, R. J. Structure and Magnetic Properties of the Spin-1/2-Based Honeycomb $NaNi_2BiO_{6-\delta}$ and Its Hydrate $NaNi_2BiO_{6-\delta} \cdot 1.7H_2O$. *Inorg. Chem.* **2014**, *53* (20), 10989–10995.

(6) Takada, K.; Sakurai, H.; Takayama-Muromachi, E.; Izumi, F.; Dilanian, R. A.; Sasaki, T. Superconductivity in Two-Dimensional CoO_2 Layers. *Nature* **2003**, *422* (6927), 53–55.

(7) Greaves, C.; Katib, S. M. A. The Structural Chemistry of $Li_3Zn_2MO_6$ (M=Sb, Bi) and Related Phases. *Mater. Res. Bull.* **1990**, *25* (9), 1175–1182.

(8) Wong, C.; Avdeev, M.; Ling, C. D. Zig-Zag Magnetic Ordering in Honeycomb-Layered $Na_3Co_2SbO_6$. *J. Solid State Chem.* **2016**, *243*, 18–22.

(9) Zvereva, E. A.; Evstigneeva, M. A.; Nalbandyan, V. B.; Savelieva, O. A.; Ibragimov, S. A.; Volkova, O. S.; Medvedeva, L. I.; Vasiliev, A. N.; Klingeler, R.; Buechner, B. Monoclinic Honeycomb-Layered Compound $Li_3Ni_2SbO_6$: Preparation, Crystal Structure and Magnetic Properties. *Dalton Trans.* **2011**, *41* (2), 572–580.

(10) Zhong, J.; Chen, X.; Chen, D.; Liu, M.; Zhu, Y.; Li, X.; Ji, Z. A Novel Rare-Earth Free Red-Emitting $Li_3Mg_2SbO_6$:Mn4+ Phosphor-in-Glass for Warm w-LEDs: Synthesis, Structure, and Luminescence Properties. *J. Alloys Compd.* **2019**, *773*, 413–422.

(11) Yuan, D.; Liang, X.; Wu, L.; Cao, Y.; Ai, X.; Feng, J.; Yang, H. A Honeycomb-Layered $Na_3Ni_2SbO_6$: A High-Rate and Cycle-Stable Cathode for Sodium-Ion Batteries. *Adv. Mater.* **2014**, *26* (36), 6301–6306.

(12) Xu, J.; Assoud, A.; Soheilnia, N.; Derakhshan, S.; Cuthbert, H. L.; Greedan, J. E.; Whangbo, M. H.; Kleinke, H. Synthesis, Structure, and Magnetic Properties of the Layered Copper(II) Oxide $Na_2Cu_2TeO_6$. *Inorg. Chem.* **2005**, *44* (14), 5042–5046.

(13) Viciu, L.; Huang, Q.; Morosan, E.; Zandbergen, H. W.; Greenbaum, N. I.; McQueen, T.; Cava, R. J. Structure and Basic Magnetic Properties of the Honeycomb Lattice Compounds $Na_2Co_2TeO_6$ and $Na_3Co_2SbO_6$. *J. Solid State Chem.* **2007**, *180* (3), 1060–1067.

(14) Uma, S.; Gupta, A. Synthesis and Characterization of New Rocksalt Superstructure Type Layered Oxides $Li_{4.5}M_{0.5}TeO_6$ (M(III)=Cr, Mn, Al, Ga). *Mater. Res. Bull.* **2016**, *76*, 118–123.

(15) Smirnova, O. A.; Nalbandyan, V. B.; Petrenko, A. A.; Avdeev, M. Subsolidus Phase Relations in Na_2O–CuO–Sb_2O_n System and Crystal Structure of New Sodium Copper Antimonate $Na_3Cu_2SbO_6$. *J. Solid State Chem.* **2005**, *178* (4), 1165–1170.

(16) Skakle, J. M. S.; Castellanos R., M. A.; Tovar, S. T.; West, A. R. Synthesis of $Li_3Cu_2SbO_6$, a New Partially Ordered Rock Salt Structure. *J. Solid State Chem.* **1997**, *131* (1), 115–120.

(17) Seibel, E. M.; Roudebush, J. H.; Wu, H.; Huang, Q.; Ali, M. N.; Ji, H.; Cava, R. J. Structure and Magnetic Properties of the A-$NaFeO_2$-Type Honeycomb Compound $Na_3Ni_2BiO_6$. *Inorg. Chem.* **2013**, *52* (23), 13605–13611.

(18) Nalbandyan, V. B.; Avdeev, M.; Evstigneeva, M. A. Crystal Structure of Li_4ZnTeO_6 and Revision of $Li_3Cu_2SbO_6$. *J. Solid State Chem.* **2013**, *199*, 62–65.

(19) Kumar, V.; Gupta, A.; Uma, S. Formation of Honeycomb Ordered Monoclinic $Li_2M_2TeO_6$ (M = Cu, Ni) and Disordered Orthorhombic $Li_2Ni_2TeO_6$ Oxides. *Dalton Trans.* **2013**, *42* (42), 14992–14998.

(20) Kumar, V.; Bhardwaj, N.; Tomar, N.; Thakral, V.; Uma, S. Novel Lithium-Containing Honeycomb Structures. *Inorg. Chem.* **2012**, *51* (20), 10471–10473.

(21) Deng, Z.; Gu, J.; Li, Y.; Li, S.; Peng, J.; Li, X.; Luo, J.; Huang, Y.; Fang, C.; Li, Q.; et al. Ca-Doped $Na_2Zn_2TeO_6$ Layered Sodium Conductor for All-Solid-State Sodium-Ion Batteries. *Electrochimica Acta* **2019**, *298*, 121–126.

(22) Berthelot, R.; Schmidt, W.; Muir, S.; Eilertsen, J.; Etienne, L.; Sleight, A. W.; Subramanian, M. A. New Layered Compounds with Honeycomb Ordering: $Li_3Ni_2BiO_6$, $Li_3NiM'BiO_6$ (M′ = Mg, Cu, Zn), and the Delafossite $Ag_3Ni_2BiO_6$. *Inorg. Chem.* **2012**, *51* (9), 5377–5385.

(23) Berthelot, R.; Schmidt, W.; Sleight, A. W.; Subramanian, M. A. Studies on Solid Solutions Based on Layered Honeycomb-Ordered Phases P2-$Na_2M_2TeO_6$ (M=Co, Ni, Zn). *J. Solid State Chem.* **2012**, *196*, 225–231.

(24) Mather, G. C.; Smith, R. I.; Skakle, J. M. S.; Fletcher, J. G.; R, M. A. C.; Gutierrez, M. P.; West, A. R. Synthesis and Structures of the Partially Ordered Rock Salt Phases, $Li_3M_2XO_6$: M=Mg, Co, Ni; X=Nb, Ta, Sb. *J. Mater. Chem.* **1995**, *5* (8), 1177–1182.

(25) Fletcher, J. G.; Mather, G. C.; West, A. R.; Castellanos, M.; Gutierrez, M. P. $Li_3Ni_2TaO_6$: A Novel Rock Salt Superstructure Phase with Partial Cation Order. *J. Mater. Chem.* **1994**, *4* (8), 1303–1305.

(26) Mather, G. C.; Dussarrat, C.; Etourneau, J.; West, A. R. A Review of Cation-Ordered Rock Salt Superstructureoxides. *J. Mater. Chem.* **2000**, *10* (10), 2219–2230.

(27) Heymann, G.; Selb, E.; Kogler, M.; Götsch, T.; Köck, E.-M.; Penner, S.; Tribus, M.; Janka, O. $Li_3Co_{1.06(1)}TeO_6$: Synthesis, Single-Crystal Structure and Physical Properties of a New Tellurate Compound with CoII/CoIII Mixed Valence and Orthogonally Oriented Li-Ion Channels. *Dalton Trans.* **2017**, *46* (37), 12663–12674.

(28) Masese, T.; Yoshii, K.; Yamaguchi, Y.; Okumura, T.; Huang, Z.-D.; Kato, M.; Kubota, K.; Furutani, J.; Orikasa, Y.; Senoh, H.; et al. Rechargeable Potassium-Ion Batteries with Honeycomb-Layered Tellurates as High Voltage Cathodes and Fast Potassium-Ion Conductors. *Nat. Commun.* **2018**, *9* (1), 3823.

(29) Bera, A. K.; Yusuf, S. M.; Kumar, A.; Ritter, C. Zigzag Antiferromagnetic Ground State with Anisotropic Correlation Lengths in the Quasi-Two-Dimensional Honeycomb Lattice Compound $Na_2Co_2TeO_6$. *Phys. Rev. B* **2017**, *95* (9), 094424.

(30) Liu, H.; Khaliullin, G. Pseudospin Exchange Interactions in d^7 Cobalt Compounds: Possible Realization of the Kitaev Model. *Phys. Rev. B* **2018**, *97* (1), 014407.

(31) Skakle, J. M. S.; R, M. A. C.; Tovar, S. T.; Fray, S. M.; West, A. R. The Crystal Structure of Li_3SbO_4. *J. Mater. Chem.* **1996**, *6* (12), 1939–1942.

(32) Blasse, G. New Types of Cation-Order in the Rocksalt Lattice: The Structure of Li_3SbO_4 and Li_3NbO_4. *Z. Für Anorg. Allg. Chem.* **1963**, *326* (1–2), 44–46.

(33) Järvinen, M. Application of Symmetrized Harmonics Expansion to Correction of the Preferred Orientation Effect. *J. Appl. Crystallogr.* **1993**, *26* (4), 525–531.

(34) Coelho, A. A. TOPAS and TOPAS-Academic: An Optimization Program Integrating Computer Algebra and Crystallographic Objects Written in C++. *J. Appl. Crystallogr.* **2018**, *51* (1), 210–218.

(35) Brese, N. E.; O'keeffe, M. Bond-Valence Parameters for Solids. *Acta Crystallogr. B* **1991**, *47* (2), 192–197.

(36) Liu, J.; Yin, L.; Wu, L.; Bai, J.; Bak, S.-M.; Yu, X.; Zhu, Y.; Yang, X.-Q.; Khalifah, P. G. Quantification of Honeycomb Number-Type Stacking Faults: Application to $Na_3Ni_2BiO_6$ Cathodes for Na-Ion Batteries. *Inorg. Chem.* **2016**, *55* (17), 8478–8492.

(37) Shunmugasundaram, R.; Arumugam, R. S.; Dahn, J. R. A Study of Stacking Faults and Superlattice Ordering in Some Li-Rich Layered Transition Metal Oxide Positive Electrode Materials. *J. Electrochem. Soc.* **2016**, *163* (7), A1394–A1400.

(38) Lefrançois, E.; Songvilay, M.; Robert, J.; Nataf, G.; Jordan, E.; Chaix, L.; Colin, C. V.; Lejay, P.; Hadj-Azzem, A.; Ballou, R.; et al. Magnetic Properties of the Honeycomb Oxide $Na_2Co_2TeO_6$. *Phys. Rev. B* **2016**, *94* (21), 214416.

(39) Yuan, D.; Liang, X.; Wu, L.; Cao, Y.; Ai, X.; Feng, J.; Yang, H. A Honeycomb-Layered $Na_3Ni_2SbO_6$: A High-Rate and Cycle-Stable Cathode for Sodium-Ion Batteries. *Adv. Mater.* **2014**, *26* (36), 6301–6306.

(40) Ma, J.; Bo, S.-H.; Wu, L.; Zhu, Y.; Grey, C. P.; Khalifah, P. G. Ordered and Disordered Polymorphs of $Na(Ni_{2/3}Sb_{1/3})O_2$: Honeycomb-Ordered Cathodes for Na-Ion Batteries. *Chem. Mater.* **2015**, *27* (7), 2387–2399.

(41) Gupta, A.; Buddie Mullins, C.; Goodenough, J. B. $Na_2Ni_2TeO_6$: Evaluation as a Cathode for Sodium Battery. *J. Power Sources* **2013**, *243*, 817–821.

(42) Sathiya, M.; Ramesha, K.; Rousse, G.; Foix, D.; Gonbeau, D.; Guruprakash, K.; Prakash, A. S.; Doublet, M. L.; Tarascon, J.-M. Li_4NiTeO_6 as a Positive Electrode for Li-Ion Batteries. *Chem. Commun.* **2013**, *49* (97), 11376–11378.

(43) Zvereva, E. A.; Nalbandyan, V. B.; Evstigneeva, M. A.; Koo, H.-J.; Whangbo, M.-H.; Ushakov, A. V.; Medvedev, B. S.; Medvedeva, L. I.; Gridina, N. A.; Yalovega, G. E.; et al. Magnetic and Electrode Properties, Structure and Phase Relations of the Layered Triangular-Lattice Tellurate Li_4NiTeO_6. *J. Solid State Chem.* **2015**, *225*, 89–96.

(44) Berthelot, R.; Schmidt, W.; Muir, S.; Eilertsen, J.; Etienne, L.; Sleight, A. W.; Subramanian, M. A. New Layered Compounds with Honeycomb Ordering: $Li_3Ni_2BiO_6$, $Li_3NiM'BiO_6$ (M′ = Mg, Cu, Zn), and the Delafossite $Ag_3Ni_2BiO_6$. *Inorg. Chem.* **2012**, *51* (9), 5377–5385.

Other files

HC.cif (0.97 KiB)	view on ChemRxiv • download file
RS.cif (1.67 KiB)	view on ChemRxiv • download file